



OPEN

SUBJECT AREAS:

FLUORESCENCE
IMAGING

CELL-CYCLE EXIT

Received
19 August 2013Accepted
17 January 2014Published
6 February 2014

Correspondence and
requests for materials
should be addressed to
T.K. (kitamura@ims.u-
tokyo.ac.jp) or T.O.
(toki+ky@umin.ac.jp)

A novel cell-cycle-indicator, mVenus-p27K⁻, identifies quiescent cells and visualizes G0–G1 transition

Toshihiko Oki^{1,2}, Koutarou Nishimura¹, Jiro Kitaura¹, Katsuhiko Togami¹, Akie Maehara¹, Kumi Izawa¹, Asako Sakaue-Sawano^{3,4}, Atsushi Niida⁵, Satoru Miyano^{5,6}, Hiroyuki Aburatani⁷, Hiroshi Kiyonari⁸, Atsushi Miyawaki^{3,4} & Toshio Kitamura^{1,2}

¹Division of Cellular Therapy, The Institute of Medical Science, The University of Tokyo, Minato-ku, Tokyo 108-8639, Japan, ²Division of Stem Cell Signaling, The Institute of Medical Science, The University of Tokyo, 4-6-1 Shirokanedai, Minato-ku, Tokyo 108-8639, Japan, ³Laboratory for Cell Function and Dynamics, Advanced Technology Development Group, Brain Science Institute, RIKEN, ⁴Life Function and Dynamics, ERATO, JST, 2-1 Hirosawa, Wako-city, Saitama 351-0198, Japan, ⁵Laboratory of DNA Information Analysis, Human Genome Center, The Institute of Medical Science, The University of Tokyo, Minato-ku, Tokyo 108-8639, Japan, ⁶Laboratory of Sequence Analysis, Human Genome Center, The Institute of Medical Science, The University of Tokyo, 4-6-1 Shirokanedai Minato-ku, Tokyo 108-8639, Japan, ⁷Genome Science Division, Research Center for Advanced Science and Technology, The University of Tokyo, 4-6-1 Komaba, Meguro-ku, Tokyo 153-8904, Japan, ⁸Laboratory for Animal Resources and Genetic Engineering, RIKEN Center for Developmental Biology, 2-2-3 Minatojima Minamimachi, Chuoku, Kobe, Hyogo, 650-0047, Japan.

The quiescent (G0) phase of the cell cycle is the reversible phase from which the cells exit from the cell cycle. Due to the difficulty of defining the G0 phase, quiescent cells have not been well characterized. In this study, a fusion protein consisting of mVenus and a defective mutant of CDK inhibitor, p27 (p27K⁻) was shown to be able to identify and isolate a population of quiescent cells and to effectively visualize the G0 to G1 transition. By comparing the expression profiles of the G0 and G1 cells defined by mVenus-p27K⁻, we have identified molecular features of quiescent cells. Quiescence is also an important feature of many types of stem cells, and mVenus-p27K⁻-transgenic mice enabled the detection of the quiescent cells with muscle stem cell markers in muscle in vivo. The mVenus-p27K⁻ probe could be useful in investigating stem cells as well as quiescent cells.

Mammalian cells are known to exit the cell cycle in response to environmental changes such as depletion of nutrition or growth factors, changes in cell adhesion, and increased cell density during the early G1 phase^{1–5}. This state is called the quiescent or the G0 phase. Many types of differentiated cells are found in the G0 phase in vivo and quiescence is also an important feature of stem cells such as hematopoietic^{6–10}, muscle^{11–15}, intestinal¹⁶, and epithelial¹⁷ stem cells.

Cells in the G0 phase have not been well characterized. The quiescent cells have been considered to be dormant, waiting to enter the cell cycle^{3–5}. Recently, several reports have challenged this notion, suggesting that quiescence is more dynamic^{3–5}.

Many approaches to distinguishing the living cells in the G0 phase from the cycling cells have been developed and are being studied extensively^{6–9,18}. However, the distinction between the G0 and G1 phase has been questioned¹⁹, as the cell-cycle transition from the G0 to G1 phase has been difficult to visualize.

As reported in previous studies, we developed a fluorescent protein-based indicator system to monitor the cell cycle status, called the fluorescent ubiquitination-based cell cycle indicator (Fucci)^{20,21}. In this system, G1 phase-specific proteolysis of Geminin and S/G2/M phase-specific proteolysis of Cdt1 are monitored using two kinds of probes consisting of the fusion proteins between the degrons of Geminin and of Cdt1 to fluorescent proteins. The Fucci system differentially labels the cells in the G1 phase and those in S/G2/M phase, effectively visualizing the G1-S and M-G1 transitions. However, Fucci cannot be used to distinguish the cells in the G0 phase from those in the G1 phase, since Cdt1 is expressed in both phases²⁰.

A cyclin-dependent kinase (CDK) inhibitor, p27 inhibits CDK1, 2, 4, and 6 via interaction with Cyclin-CDK complex²² and inhibits cell cycle progression at the G0–G1 and G1-S transitions^{23–26}. Its expression is strictly regulated by at least two kinds of ubiquitin ligases; KPC promotes proteolysis of p27 at G0–G1 transition²⁷, and



SCF^{Skp2} promotes its proteolysis at the S/G2/M phase^{28,29}. The levels of p27 are higher in quiescent cells than in cycling cells^{30–33}.

In the present study, to visualize the cells in the G0 phase, we transduced a probe, using a fusion protein between the fluorescent protein mVenus and a p27K⁻ mutant lacking CDK inhibitory activity (mVenus-p27K⁻) to NIH3T3 cells. The expression of mVenus-p27K⁻ was observed mainly in the cells of the G0 phase and was also detected in the cells in early G1. However, this marker was able to identify and isolate the quiescent cells. In addition, the cells in the G0 phase were distinguished from those in G1 during the G0–G1 transition with a combination of mVenus-p27K⁻ and Fucci probes. Expression profiles of the cells in the G0 phase revealed that they expressed a set of genes related to cell metabolism, inflammatory response, epigenetics and tumor suppression. These molecular features are consistent with the nature of quiescent cells as recently reported, supporting the feasibility of our system. Studies using transgenic mice with mVenus-p27K⁻ revealed that this marker was useful for detecting the quiescent cell population in skeletal muscle with the markers of muscle stem cells. These findings indicate that the mVenus-p27K⁻ probe is a useful tool in investigating stem cell biology as well as the mechanisms maintaining quiescence.

Results

Development of an mVenus-p27K⁻ probe that identifies quiescent cells. To develop fluorescent probes that visualize the cells in the G0 phase, we first fused mVenus to the N-terminus of wild type p27 and retrovirally transduced the resulting fusion protein (mVenus-p27WT) to NIH3T3 cells. However, stably transduced cells with mVenus-p27WT were not established, probably due to the CDK inhibitory function of p27.

p27 has two functional domains, the cyclin binding domain and the Cdk binding domain. The mutations that block the binding affinity in either or both of these domains are reported to be devoid of the CDK-cyclin inhibitory activity of p27³⁴. Therefore, we next fused p27 mutants that lack binding affinity to cyclin (p27C⁻), Cdk (p27K⁻), or both (p27CK⁻) to mVenus (Fig. 1A). These probes were retrovirally transduced to NIH3T3 cells. All of the transduced cells were able to proliferate and their stably transduced cells were established (Fig. 1B and Fig. S1–3). Our initial studies showed that the brighter fluorescent emission was observed in the mVenus-p27C⁻ or mVenus-p27CK⁻ transduced cells than in mVenus-p27K⁻ transduced cells (Fig. 1B), due to its susceptibility for ubiquitin-mediated degradation as reported³⁴. However, the expression of mVenus-p27C⁻ or mVenus-p27CK⁻ was observed in the S/G2/M phase in addition to the G1 phase. On the other hand, the expression of mVenus-p27K⁻ was confined to the G1/0 phase (Fig. 1C). Therefore, mVenus-p27K⁻ was subjected to further analysis.

The G1/0-specific probe used in Fucci2.1, mCherry-hCdt1(30/120), is expressed in both G1 and G0 cells^{20,21}. To identify the phase in which mVenus-p27K⁻ is expressed, we compared the expression of mVenus-p27K⁻ to that of mCherry-hCdt1(30/120). The cell cycle statuses of the stably transduced cells with mVenus-p27K⁻ and mCherry-hCdt1(30/120), were analyzed via Hoechst33342 staining. The distribution of each phase of the cell cycle of the transduced cells was similar to mock transduced cells (Fig. S4). The expression of mVenus-p27K⁻ and mCherry-hCdt1(30/120) was exclusively observed in the cells in the G1/0 phase (Fig. 1C). If mVenus-p27K⁻ is a marker for the cells in the G0 phase, its expression should be enriched in the G0 but not in the G1 phase. The fluorescence-activated cell sorter (FACS) analysis indicated that mVenus-p27K⁻ was expressed in this fashion. Most cells in the G1 phase expressed mCherry-hCdt1(30/120), but only half of these cells expressed mVenus-p27K⁻ (Fig. 1C left panels). On the other hand, most of the serum-starved cells, which were presumably in the G0 phase^{2–5}, expressed both markers (Fig. 1C right panels). Moreover, the expression levels of

mVenus-p27K⁻ in the serum-starved cells were 7 times greater than those in the cells in the cycling state where most cells were cycling (Fig. 1D). However, the expression levels of mCherry-hCdt1(30/120) in the serum-starved cells were only three times greater than the cells in the cycling state (Fig. 1D). Similarly, we observed enhanced expression of mVenus-p27K⁻ in the confluent cells that were in the G0 phase due to contact inhibition (Fig. S1 and data not shown). These data indicate that the mVenus-p27K⁻ probe had accumulated in the cells in G0 and that this probe could effectively detect the cells in G0 among the cells in the G1/0 phase.

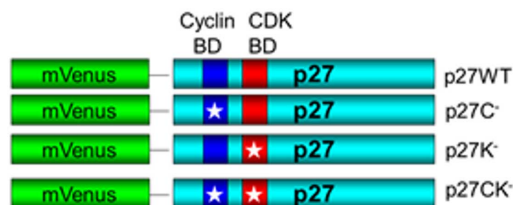
In addition, mVenus-p27K⁻ positive cells was able to isolate the Ki-67 negative population in NIH3T3 cells (Fig. 1E), and similar findings were also observed in other cell types, such as hematopoietic or lung carcinoma cells (Fig. 1F).

mVenus-p27K⁻ probes visualize the transition from the G0 to G1 phase. For a detailed cell cycle analysis of a single cell, NIH3T3 cells were transfected with mVenus-p27K⁻ in addition to Fucci2.1 G1/0 probe, mCherry-hCdt1(30/120) with or without Fucci2.1 S/G2/M probe, AmCyan-hGeminin(1/110)²¹, and subjected to time-lapse imaging. The transduced cells were cultured in a serum-free medium for 24 hr in order to let most of the cells enter the G0 phase, and then 10% fetal bovine serum (FBS) was added to the culture medium to observe the cells in the course of their entry to the cell cycle. mVenus-p27K⁻ was observed in the cells in the G0 phase at the initial phase, but also observed (albeit more weakly) in the cycling cells in the early G1 phase (Fig. 2A, B). Therefore, the mVenus-p27K⁻ probe does not solely indicate quiescent cells. In particular, this probe could not separate the cells in G0 from the cells in G1 at the time of the entering of the G0 phase (the G1–G0 transition). However, the detailed analysis of this imaging study indicated that we should be able to distinguish the cells in G0 from those in G1, at the time of the exit from the G0 phase (the G0–G1 transition). p27 is known to be ubiquitinated and targeted for degradation at the G0–G1 transition by the E3 ligase, KPC²⁷. p27 is also a substrates for another E3 ligase, SCF^{Skp2}, which is involved in p27 degradation at the G1-S transition^{28,29}. Interestingly, a G1/0-specific probe used in Fucci2.1, mCherry-hCdt1(30/120) which is also a substrate of SCF^{Skp2}, marks the cells in both the G1 and G0 phases^{20,21}. As in the cell shown as an example (Figure 2), mVenus-p27K⁻ was degraded 4–10 hr after the serum addition and mCherry-hCdt1(30/120) was degraded 8–12 hr after the serum addition along with the upregulation of Cyclin D1, Cyclin E, and Ki-67 (Fig. 2 and Fig. S5–6). The difference in the timing of the degradation between mVenus-p27K⁻ and mCherry-hCdt1(30/120) enabled us to separate the cells in G0 from the cells in G1 (Fig. 2B); the initial mVenus-p27K⁻ (+)/mCherry-hCdt1(30/120)(+) stage was considered to be the G0 phase, the following mVenus-p27K⁻ (-)/mCherry-hCdt1(30/120)(+) stage was the G1 phase and the last mVenus-p27K⁻ (-)/mCherry-hCdt1(30/120)(-) stage was to be the S/G2/M phase. Thus, we could segregate the stages in the course of cell cycle entry and clearly visualize the G0–G1 transition.

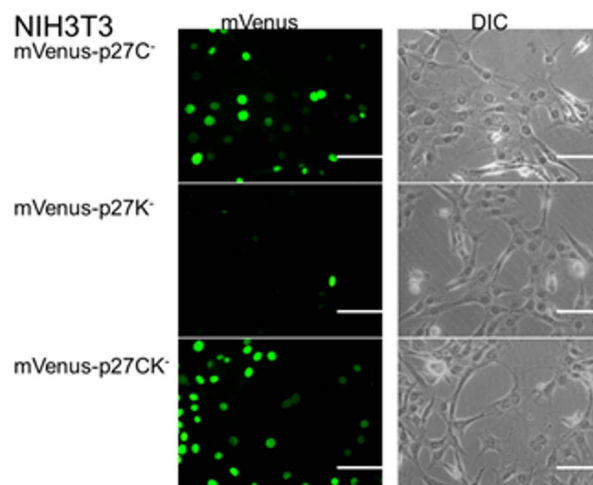
Molecular signatures for cells in the G0 phase are distinct from those for cells in the G1 phase. To examine the feasibility of our system and identify the molecular features of the cells in the G0 and G1 phases, we sorted mVenus-p27K⁻ (-)/mCherry-hCdt1(30/120) (+) NIH3T3 cells (G1 cells) and mVenus-p27K⁻ (+)/mCherry-hCdt1(30/120) (+) NIH3T3 cells (G0 cells) using FACS at 5hr after the serum addition following serum starvation (Fig. 3A). Then we performed Affymetrix-based microarray analysis and compared the results of G0 and G1 cells (Fig. 3B–D). As shown in Fig. 3B, most genes are equally expressed in G0 and G1 cells, and are thus plotted near the center line (Y = X). However some genes are plotted above or below the center line indicating these genes are differentially expressed in G0 or G1 cells.



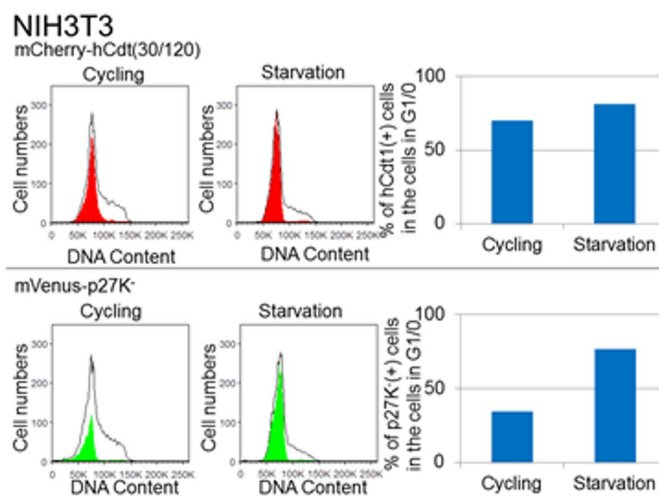
A



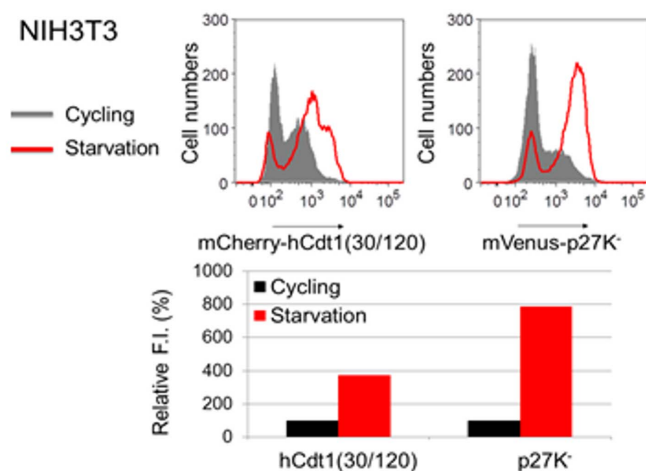
B



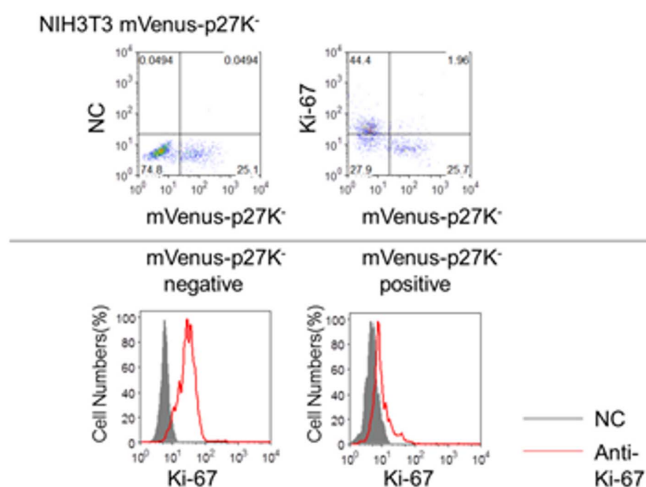
C



D



E



F

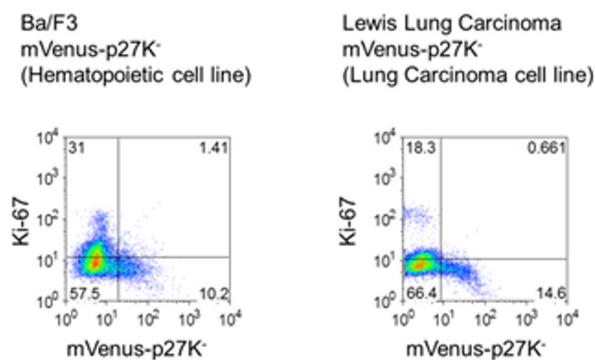


Figure 1 | mVenus-p27K⁻ probe identifies quiescent cells. (A) Various constructs with concatenated mVenus and p27. (B) Typical images of NIH3T3 transfectants (Scale, 200 μm). (C) Representative histograms for DNA contents of NIH3T3 (right) and of the fluorescent positive cells (red or green solid line), and the percentages of the fluorescent positive cells in G1/0 cells (left). (D) Representative histograms (upper) and relative median intensity (%) (Relative F.I.) (lower) of fluorescence of NIH3T3 in cycling (black) or serum starvation (red). (E–F) Representative Ki-67 staining of NIH3T3 (E) or Ba/F3 cells (F) or Lewis lung carcinoma cells (F) expressing mVenus-p27K⁻. NC, isotype control.



Several genes highly expressed in G0 cells included tumor suppressors, such as programmed cell death 4 (Pcdcd4), selenium binding protein 1 (Selenbp1) and transducer of ERBB2, 1 (Tob1) (Fig. 3C and Table S1). Ingenuity pathway analysis (IPA) revealed that the pathways of cell cycle regulators maintaining quiescence, such as TP53, cdk inhibitor 1a, 1c, 2a (CDKN1A, 1C, 2A), retinoblastoma protein 1 (RB1), and let-7, were expressed in G0 cells. These findings indicate that G0 cells indeed possess the features of quiescent cells (Table S2).

IPA and gene ontology (GO) analysis of G0 cells also revealed some additional important features of quiescent cells. According to IPA, the pathways of immune response such as interleukin 1 (IL-1), toll like receptor (TLR) 2, 3, 4, 7, 9, and nuclear factor kappa b (NFkb), and the pathway of an epigenetic modifier, lysine(K)-specific demethylase 5b (Kdm5b), were both enriched in G0 cells (Table S2). GO annotations of the genes enriched in G0 cells included inflammatory response, response to wounds, and defense response (Table S3). High metabolic rates and robust immune responses are important in maintaining quiescence²⁻⁵, and changes in the epigenetic states are reported to be required for the G0–G1 transition³⁵. The genes involved in epigenetic modification such as Kdm5b, Kdm6b, jmjC domain-containing histone demethylase 1d (Jhdm1d), and jumonji/

ARID domain-containing protein 2 (Jarid), as well as the genes in cell metabolism such as isocitrate dehydrogenase 1 (Idh1), and nuclear factor 2 (Nrf2)-were enriched in G0 cells (Fig. 3C and Table S1).

In contrast, most of the genes highly expressed in G1 cells compared to G0 cells were related to cell cycle, mitosis and proliferation, including antigen identified by monoclonal antibody ki-67 (Mki67), Aurora b, and Bub1 (Fig. 3D and Table S1). IPA revealed that the pathways of cell cycle regulators involved in the G1-S transition such as Myc, E2F and Cyclin D1 pathway were activated (Table S2). GO annotations of these genes were related to cell cycle progression and mitosis (Table S4). These findings indicate that G1 cells have features of dividing cells, and also that we could effectively separate the cells in G0 from those cells in G1 during the G0 to G1 transition.

Gene set enrichment analysis (GSEA) revealed that the expression of quiescent signature genes, such as quiescence-associated genes (Q-sig) and long term hematopoietic stem cell-associated genes (LT-HSC)⁹, was significantly increased and that the expression of proliferation signature genes, such as proliferation-associated genes (P-sig) and short term hematopoietic stem cell-associated genes (ST-HSC)⁹, was significantly decreased in G0 cells relative to G1 cells (Figure 3E).

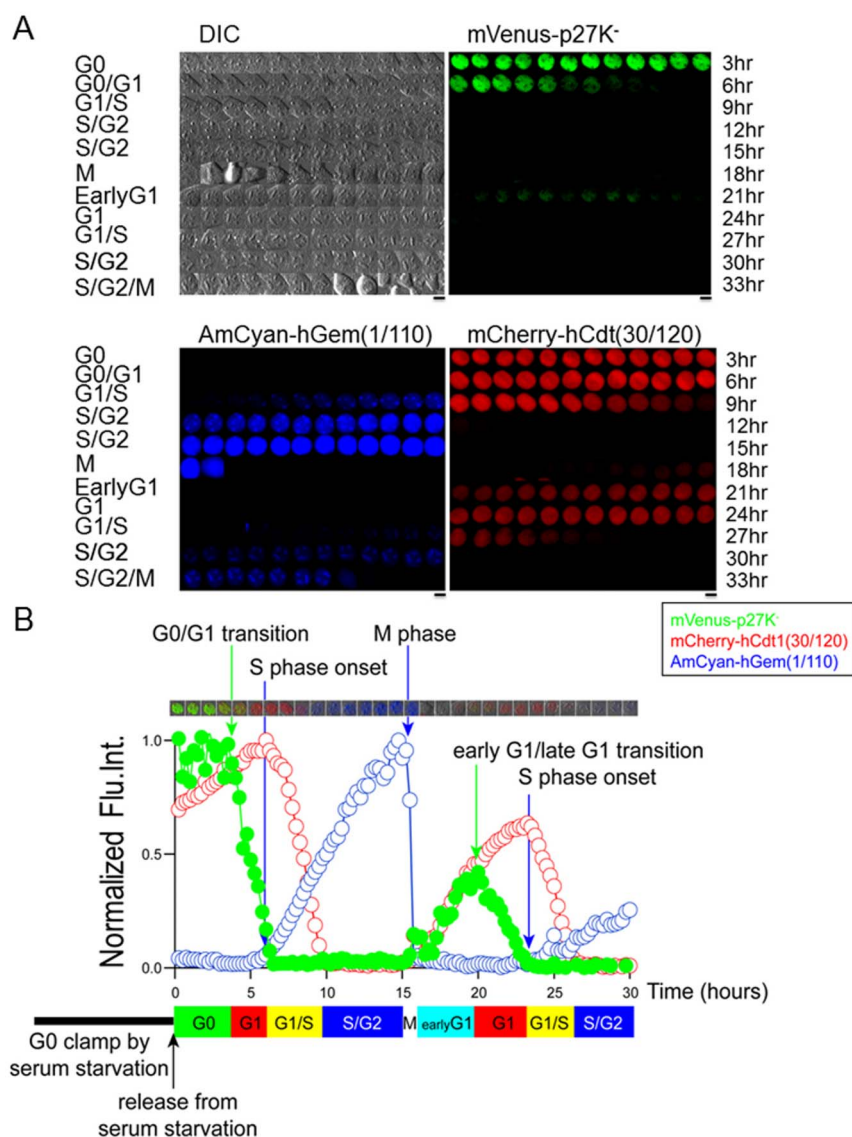


Figure 2 | mVenus-p27K⁻ and mCherry-hCdt1(30/120) probes effectively visualize G0 to G1 transition. (A) Typical images and (B) changes in normalized fluorescent intensity (Flu.Int.) of mVenus-p27K⁻, mCherry-hCdt1(30/120), and AmCyan-hGem(1/110) in NIH3T3 cells at cell cycle entry (Scale, 10 μ m).

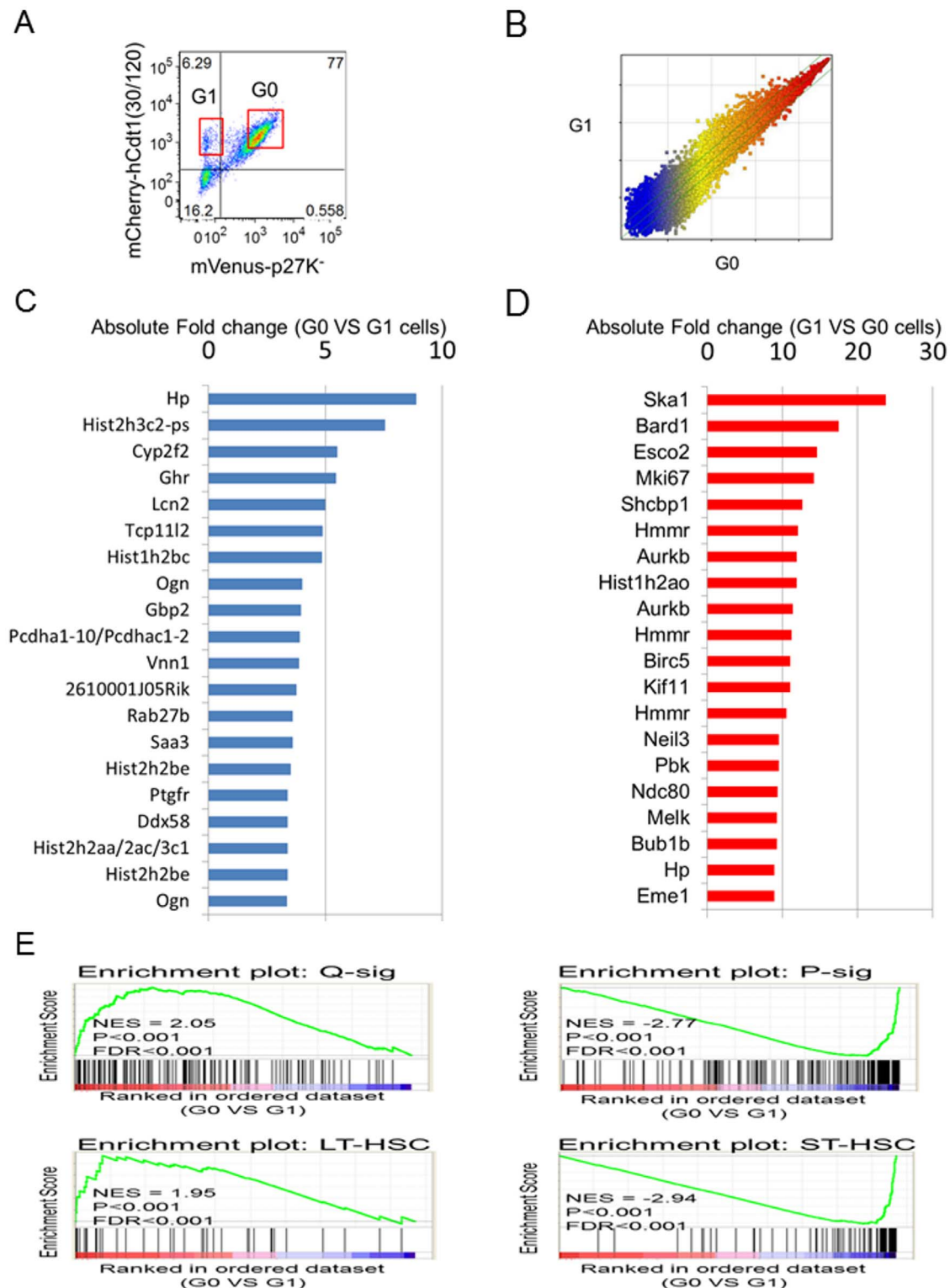


Figure 3 | Expression profiles of G0(p27K⁻)/hCdt1(30/120)(+) cells and G1((p27K⁻)/hCdt1(30/120)(+) cells. (A) FACS analysis for G0 and G1 cells. (B) Scatter plot with X and Y axis indicating the expression level of each gene in G1 and G0 cells respectively. (C–D) Catalogue of differently expressed genes: the top genes enriched (C) in G0 cells and (D) in G1 cells. (E) GSEA comparison of G0 against G1 cells. NES, normalized enrichment score; FDR, false discovery rate.

These results verified the efficacy of the mVenus-p27K⁻ probe in clearly visualizing the G0–G1 transition, and demonstrated that the molecular features of G0 cells are quite distinct from those of G1 cells.

Expression of the genes enriched in G0 cells was confirmed by quantitative RT-PCR (qPCR) (Fig. 4A). Among the genes highly

expressed in G0 cells, several are known to work as tumor suppressors, such as Pcdcd4, Selenbp1, and Tob1. The expression levels of these genes were elevated in serum-starved NIH3T3 cells, and the levels decreased in response to stimulation with serum (Fig. 4B, C). Similar results were also observed in the hematopoietic Ba/F3 cells (Fig. 4D).

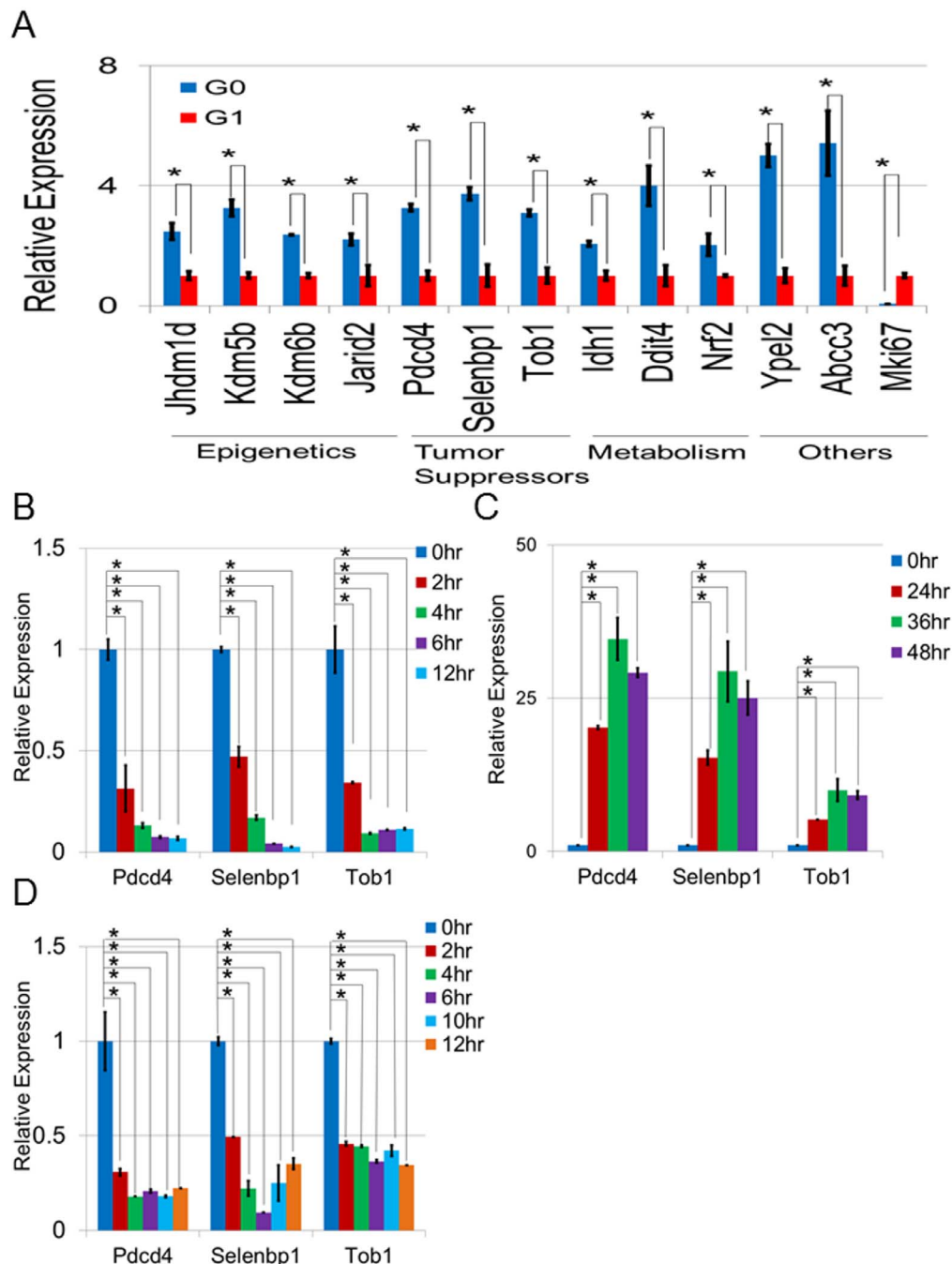


Figure 4 | Enhanced expression of several tumor suppressors was observed in the G0 phase. (A) The expression for the G0-associated genes and Mki67. (B–D) Changes in the levels of tumor suppressors in NIH3T3 cells after (B) serum addition following serum starvation or (C) serum starvation or (D) in Ba/F3 cells after the serum and IL-3 addition following their depletion. Data were analyzed by qPCR and represented as values normalized to (A) G1 cells (mean \pm S.D, n = 4) or (B–D) the levels at 0 hr (mean \pm S.D, n = 3). *, P < 0.05.

Muscle quiescent stem cell populations are visualized in mVenus-p27K⁻-transgenic mice. To analyze the behavior of the quiescent cells in vivo, we generated mVenus-p27K⁻-transgenic mice by using CAG promoter³⁶. Two germline-transmitted lines have been generated; among them, #12-2-06 with a stronger fluorescence emission was chosen for further characterization. FACS analysis revealed that the populations of mVenus-p27K⁻ positive cells were mainly observed in skeletal muscle of adult mice (Fig. 5A, B). Intriguingly, the mVenus-p27K⁻ positive population in skeletal muscle expressed CD34 and Sca-1, and no or limited expression of c-kit, CD45, CD44, and CD31 was observed (Fig. 5C). The qPCR studies revealed that the mVenus-p27K⁻ positive population in

skeletal muscle also expressed CD34, Sca-1, and Sprouty1 with much higher levels when compared to the mVenus-p27K⁻ negative population (Fig. 5D). In contrast, the expression levels of Mki67 were much lower than those found in the mVenus-p27K⁻ negative populations (Fig. 5D). Several types of muscle stem cell candidates have been reported to express CD34 and Sca-1, including muscle satellite cells¹¹ and their related progenitors³⁷ such as muscle derived stem cells (MDSC)^{11,37,38} in addition to muscle stem cells derived from hematopoietic cells³⁹. Negative expression of CD45 indicated that those cells were not of hematopoietic origin³⁹. Desmin was also expressed in the mVenus-p27K⁻ positive population, but no or limited expression of myoD,

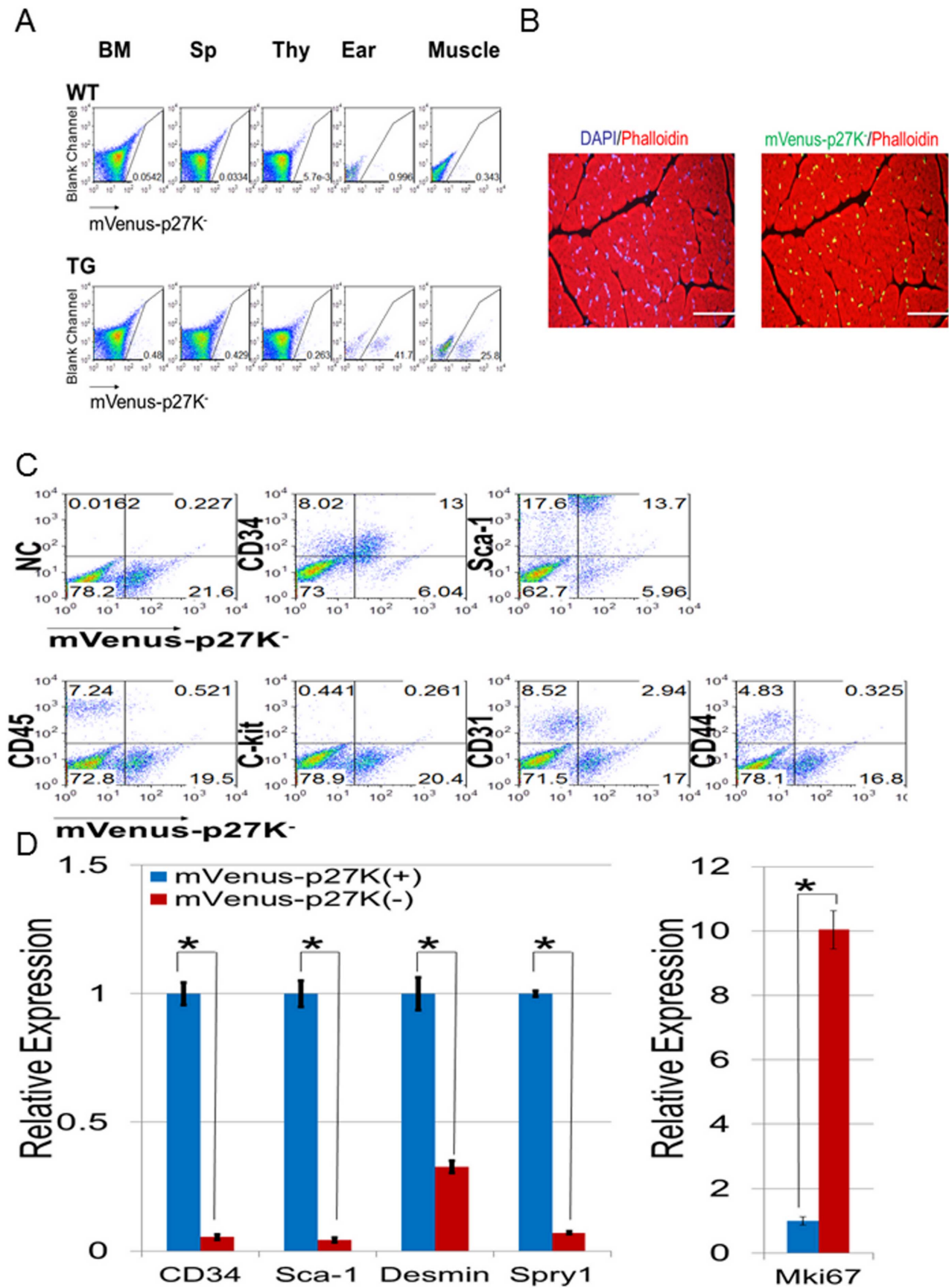


Figure 5 | mVenus-p27K⁻ positive population in skeletal muscle includes muscle satellite cells. (A) Typical FACS analysis. BM, bone marrow; Sp, spleen; Thy, thymus (B) Typical fluorescent images of sections of muscles (Scale, 200 μ m) (right). (C) FACS and (D) qPCR (mean \pm S.D., n = 3) for marker expression of muscles. *, P < 0.05.



Myogenin, Myf5, c-Met, and Pax7 was observed (Fig. 5D and data not shown), implying that mVenus-27K⁻ positive population are muscle satellite cells or related progenitor cells, MDSC^{11–13,37,38}. Muscle satellite cells are usually in the quiescent phase, but when neighboring muscles are injured, they enter the cell cycle and differentiate into mature muscle cells to regenerate the muscle tissues^{13–15}. Importantly these processes are regulated by Sprouty1^{14,15}. Higher expression of Sprouty1 and lower expression of Mki67 were observed in the mVenus-p27K⁻ positive population compared with the negative population, representing the stem cell feature of the mVenus-p27K⁻ positive population. Thus, mVenus-p27K⁻ probes could effectively detect the quiescent population in skeletal muscle which was found to express the markers of muscle stem cells.

Discussion

p27 is a target of KPC and SCF^{Skp2}. KPC is responsible for its degradation at the G0–G1 transition²⁷ and SCF^{Skp2} is responsible for its degradation at the G1–S transition^{23–26}. Thus, probes to monitor the expression of p27 are possible candidates as a marker to visualize the G0–G1 as well as the G1–S transition.

In the present study, we attempted to produce the probes using p27 mutants lacking inhibitory activity on Cyclin-CDK function. Among them, mVenus-p27K⁻ turned out to be the most promising to visualize the cells in the G0 phase. Recently, Sharma et al., have reported that the osteosarcoma cell line, U2O2 cell line transduced with p27K⁻ were unable to proliferate⁴⁰. However, the NIH3T3 cells as well as Ba/F3, LLC, 32D, and HF6⁴¹ cells transduced with mVenus-p27K⁻ proliferated normally as mock transduced cells and no obvious defect in cell cycle or cytokinesis was observed (Fig. S2–4).

Although mVenus-p27K⁻ could be detected in quiescent cells as well as in the cells in the early G1 phase, the expression levels of mVenus-p27K⁻ were quite low in early G1 cells (Fig. 2), enabling the isolation of the Ki-67-negative, quiescent population by mVenus-p27K⁻.

Several ways to identify the cells in G0 were previously developed. The retention of markers such as bromodeoxyuridine (BrdU) staining^{6–9,16,17} or histone 2B-GFP (H2B-GFP) protein^{8,10,15} has been widely used to detect the quiescent cells. Retaining these markers represents the cells with a low frequency of cell division over several weeks or months, while mVenus-p27K⁻ positive cells mainly represents the cells that did not enter the cell cycle within 4 to 10 hr. Therefore, our way of detecting the quiescent cells with mVenus-p27K⁻ would be much better in terms of temporal resolution than the traditional methods that evaluate the retention of BrdU staining or H2B-GFP protein.

Several approaches to defining the cells in G0 against the cycling cells have been proposed^{1,9,19,42}. However, a reliable means of distinguishing the G0 phase from the G1 phase has not yet been established¹⁹. Here we have presented one novel and potent way to differentiate the G0 phase from G1 phase in the course of the cell cycle entry. Using mVenus-p27K⁻ together with a G1/0 marker used in Fucci, mCherry-hCdt1(30/120), we were able to visualize the G0 to G1 transition, distinguishing the cells in G0 (G0 cells) from the cells in the G1 phase (G1 cells).

Expression profiles of G0 and G1 cells revealed that the molecular features of the G0 phase were quite distinct from those of the G1 phase. For example, microarray analysis revealed that the genes normally associated with proliferation (P-sig) were enriched in G1 cells and that the genes normally associated with the quiescent state (Q-sig) were enriched in G0 cells (Fig. 3E). In the hematopoietic system, the most immature stem cells, long-term hematopoietic stem cells (LT-HSCs), are supposed to be in G0 phase, while the relatively differentiated cells such as short-term hematopoietic stem cells (ST-LSCs) are supposed to be in the cycling state. Intriguingly, the genes associated with the LT-HSCs were also upregulated in G0 cells, while

the genes associated with the ST-HSCs were upregulated in G1 cells, suggesting that the genes differentially expressed in quiescent NIH3T3 cells are regulated by similar ways in LT-HSCs. GO annotations and the pathways of upstream regulators for the genes enriched in G1 cells were related to cell cycle progression. These findings indicate that we effectively separated the cells preceding (G0 cells) and the cells beyond (G1 cells) the restriction point of proliferation, and that monitoring the proteolysis of p27K⁻ is promising to define G0 cells against G1 cells at the G0–G1 transition.

Several pathways such as chromosomal changes, epigenetic regulations, metabolic regulations, and inflammatory responses are differentially activated in G0 cells compared to G1 cells, indicating important aspects of quiescence. The roles of epigenetic changes in the G0–G1 transition have been reported recently^{35,43}, and the genes involved in epigenetic modification (such as Kdm5b, Kdm6b, Jhdmd1 and Jarid2) are indeed upregulated in G0 cells (Fig. 4A). Quiescent cells such as the stem cells in the niche usually face a lack of nutrition or low oxygen, and metabolic regulations are required for cell survival. Metabolic genes such as Idh1, Nrf2, and Ddit4 were highly expressed in G0 cells. These genes are also important in quiescence. For example, Idh1, which is responsible for NADPH production, is a key metabolic enzyme in quiescent human fibroblast³, and Nrf2, which works as an important factor in protection from oxidative stress, has recently been reported to play a pivotal role in maintaining hematopoietic stem cells⁴⁴. As reported⁴, elevated immune response is one of the characteristics of quiescence. Thus, our mVenus-p27K⁻ marker gives a molecular basis for substantial differences between the cells in the G0 and G1 phases, indicating the feasibility of our system.

We also identified several tumor suppressors, such as Pcd4, Selnebp1 and Tob1 enriched in G0 cells (Fig. 4A–D). Interestingly the diminished expression levels of these genes are correlated with poor prognosis of malignancies^{45–47}. Therefore, these genes are thought to possess some growth inhibitory effects, and the combined functions of these tumor suppressors may turn out to be required for the maintenance of quiescence.

Analysis of the transgenic mice with mVenus-p27K⁻ revealed that mVenus-p27K⁻ positive cells were mainly observed in skeletal muscle. The positive cells in skeletal muscle expressed CD34, Sca-1, Desmin, and Sprouty1, but only limited amounts of myogenin, MyoD, Myf5, c-Met, Pax7, and CD31, and did not express CD44 or CD45. The expression levels of Mki67 were lower in the mVenus-p27K⁻ positive population than those in the negative populations, implying that the positive cells are muscle satellite cells or their related progenitors^{13–15}, which have muscle stem cell-activity and are normally in quiescence.

Many types of tissue-specific stem cells are found in the G0 phase, such as hematopoietic stem cells (HSC) or neural stem cells (NSC) as well as muscle stem cells. Findings from the transgenic mice indicate their potential as a tool to detect stem cells other than muscle stem cells, such as HSC and NSC in vivo. However, the expression of mVenus-p27K⁻ was low or undetectable in hematopoietic and neural cells in the transgenic mice studied. Therefore, to investigate HSC or NSC, we need to establish other lines of transgenic mice or transgenic mice using different promoters. Nonetheless, mVenus-p27K⁻ appears to be a powerful tool in stem cell biology.

Methods

Plasmids. cDNA for hGeminin(1/110) and hCdt1(30/120) were amplified by PCR from pCSII-MCS-mVenus-hGeminin(1/110) and pCSII-MCS-mCherry-hCdt1(30/120)^{21,48} using primers with 5'-XhoI and 3'-NotI sites and subcloned into pMXs vector⁴⁹. Mouse p27 was amplified from mouse bone marrow cDNA using primers with 5'-XhoI and 3'-NotI sites by PCR. The p27 mutants, p27C⁻ (p27-R30A-L32A), p27K⁻ (p27-F62A-F64A), p27CK⁻ (p27-R30A-L32A-F62A-F64A) were generated by PCR-based mutagenesis as reported³⁴. These fragments were subcloned into a pMXs-internal ribosome entry site (IRES)-Puro vector (pMXs-IP) (Step1). All constructs were verified by DNA sequencing. The fragments for mVenus, mCherry, and AmCyan were digested from pCSII-MCS-mVenus-hGeminin(1/110),



pCSII-MCS-mCherry-hGemini(1/110), and pCSII-MCS-AmCyan-hGemini(1/110)⁴⁶ by EcoRI and XhoI, respectively and subcloned into the plasmids described in Step 1,

to make pMXs-mVenus-hGemini(1/110), pMXs-mCherry-hGemini(1/110), pMXs-AmCyan-hGemini(1/110), pMXs-mCherry-hCdt1(30/120), pMXs-IP-mVenus-p27⁻, pMXs-IP-mVenus-p27C⁻, pMXs-IP-mVenus-p27K⁻, and pMXs-IP-mVenus-p27CK⁻ (Step 2).

Cell culture. NIH3T3 cells were cultured in DMEM supplemented with 10% FBS and penicillin/streptomycin (DMEM/10%FBS). For Plat-E cells, DMEM/10%FBS supplemented with 1 µg/ml puromycin and 10 µg/ml blasticidin was used⁵⁰. For the serum starvation and serum addition (release), the cells were cultured in DMEM supplemented with 0.1% BSA, 10 mM HEPES, and penicillin/streptomycin (starvation medium) for 24 hr or more and the culture medium was replaced with DMEM/10%FBS. Ba/F3 cells were cultured in RPMI supplemented with 1 ng/ml IL-3, 10% FBS and penicillin/streptomycin. To deplete serum and IL-3, Ba/F3 cells were cultured in RPMI supplemented with 0.1% BSA, 10 mM HEPES, and penicillin/streptomycin for 24 hr.

Retroviral transduction. Retrovirus infection was performed as described previously^{49,50}. Briefly, retroviruses were generated by transient transfection to Plat-E cells by the calcium phosphate method and used for the infection to NIH3T3 cells. The transduced NIH3T3 cells were subjected to drug selection with 1 µg/ml puromycin or the selection of fluorescent positive cells by FACS sorting.

Flow cytometry. Briefly, cells were stained with the following phycoerythrin-conjugated antibodies (Abs) CD34, Sca-1, CD45, c-kit, CD31, CD44 (BD Biosciences) and Ki-67 (eBiosciences) or Hoechst 33342 solution (Invitrogen). Flow cytometric analysis was performed by FACSCalibur or FACSARIA II (BD Biosciences) and analyzed by FlowJo (Tree Star).

For sorting G0 and G1 cells, the transduced NIH3T3 cells were cultured in DMEM supplemented with 10% FBS for 5 hr after they were cultured in starvation medium. mVenus-p27K⁻(+)/mCherry-hCdt1(30/120)(+) NIH3T3 cells (G0) or mVenus-p27K⁻(-)/mCherry-hCdt1(30/120)(+) NIH3T3 cells (G1) were sorted using FACS ARIA II.

Real-time PCR analysis. Real-time PCR was performed as described previously⁵¹. cDNA generated from total RNA was mixed with SYBR Green (TAKARA). The reaction was subjected to a treatment cycle at 95°C for 30 s followed by 45 cycles for PCR at for 5 s, at 55°C for 10 s and at 72°C for 10 s. The primer pairs are described in the supplementary information (Table S5).

Imaging study. Imaging studies were conducted as described previously^{20,21}. Briefly, cells cultured on a 35-mm glass-bottom dish in DMEM/10%FBS were subjected to time-lapse imaging by LCV100 (Olympus) with an objective lens (X40). An image was acquired every 15 minutes until the end of the observation. Image acquisition and analysis were performed with MetaMorph (Universal Imaging). The cells were cultured in starvation medium for 24 hr before imaging, if required.

Microarray analysis. Total RNA from sorted G0 and G1 cells was extracted with TRIzol (Invitrogen), and 100 ng or 1 µg of total RNA was used to produce biotinylated cRNA. Then the biotinylated cRNA was hybridized to Genechip[®] Mouse Genome430 2.0 (Affymetrix) microarrays and analyzed as described previously^{52,53}. The data were analyzed with Microarray Suite version 5.0 (MAS 5.0) using Affymetrix default analysis settings and global scaling as normalization method, and G0 and G1 cells were compared by GeneSpring (Agilent Technologies). The genes upregulated in G0 or G1 cells were annotated for their associated biological processes with the Database for Annotation, Visualization, and Integrated Discovery (DAVID) (<http://david.abcc.ncicrf.gov/>). The pathway analysis of upstream regulators was conducted by IPA (Ingenuity). Normalized data were filtered for minimal fold change and GSEA⁵⁴ (<http://www.broadinstitute.org/gsea/index.jsp>) was conducted as described elsewhere⁵³. For GSEA analysis, the gene sets were derived from Venezia et al⁹. For a gene to be considered significantly increased or repressed, the fold difference should be >1.5. The results of GO annotation and IPA were filtered for statistical significance using the nominal p value < 0.001. The results of GSEA were filtered for statistical significance using the nominal p value threshold of 0.01. The normalized data set of this analysis can be obtained at the Gene Expression Omnibus site (<http://www.ncbi.nlm.nih.gov/geo/>) (GEO accession code: GSE46511).

Generation of transgenic mice. cDNA encoding mVenus-p27K⁻ was cloned into a pCAGGS vector⁵¹. An insert including CAG promoter, mVenus-p27K⁻, and polyA was digested from the vector and microinjected into zygotes of C57BL/6 inbred mice. Screening of transgenic mice was performed by genotyping. Primers used for genotyping were as follows: forward primer-1, 5'-tacaactacaacgccaacg-3'; reverse primer-1, 5'-atgattctggcgctggcattcactcg-3'; forward primer-2, 5'-caagatccgcaacatcg-3'; reverse primer-2, 5'-gggcttctggcctctgtccac-3', and target sizes for primer set 1 and 2 for genotyping were 518 bp and 822 bp, respectively.

Two lines were germ line transmitted (Acc. No.CDB0486T:<http://www.cdb.riken.jp/arg/TG%20mutant%20mice%20list.html>). One line (#12-2-6) with the strongest emission was selected for further evaluation. To isolate the ear and muscle cells, tissue samples from the ears or the muscles of hind limbs were treated with type I

collagenase (Invitrogen), filtered, and collected in culture medium as described elsewhere⁵⁶. The cells were then subjected to FACS analysis or RNA extraction by RNeasy Mini Kit (Qiagen). All animal studies were approved by the Animal Care Committees of the Institute of Medical Science, the University of Tokyo, and the RIKEN Center for Developmental Biology.

Statistical analysis. Statistical significance was calculated using the Student *t* test (one way) for independent variables. *P* values < .05 were considered statistically significant.

- Zetterberg, A. & Larsson, O. Kinetic analysis of regulatory events in G1 leading to proliferation or quiescence of Swiss 3T3 cells. *Proc Natl Acad Sci U S A* **82**, 5365–5369 (1985).
- Coller, H. A., Sang, L. & Roberts, J. M. A new description of cellular quiescence. *PLoS Biol* **4**, e83 (2006).
- Lemons, J. M. et al. Quiescent fibroblasts exhibit high metabolic activity. *PLoS Biol* **8**, e1000514 (2010).
- Chen, B. R. et al. Quiescent fibroblasts are more active in mounting robust inflammatory responses than proliferative fibroblasts. *PLoS One* **7**, e49232 (2012).
- Legesse-Miller, A. et al. Quiescent fibroblasts are protected from proteasome inhibition-mediated toxicity. *Mol Biol Cell* **23**, 3566–3581 (2012).
- Zhang, J. et al. Identification of the haematopoietic stem cell niche and control of the niche size. *Nature* **425**, 836–841 (2003).
- Arai, F. et al. Tie2/angiopoietin-1 signaling regulates hematopoietic stem cell quiescence in the bone marrow niche. *Cell* **118**, 149–161 (2004).
- Foudi, A. et al. Analysis of histone 2B-GFP retention reveals slowly cycling hematopoietic stem cells. *Nat Biotechnol* **27**, 84–90 (2009).
- Venezia, T. A. et al. Molecular signatures of proliferation and quiescence in hematopoietic stem cells. *PLoS Biol* **2**, e301 (2004).
- Sugimura, R. et al. Noncanonical Wnt signaling maintains hematopoietic stem cells in the niche. *Cell* **150**, 351–365 (2012).
- Gharabeh, B. et al. Isolation of a slowly adhering cell fraction containing stem cells from murine skeletal muscle by the preplate technique. *Nat Protoc* **3**, 1501–1509 (2008).
- Tanaka, K. K. et al. Syndecan-4-expressing muscle progenitor cells in the SP engraft as satellite cells during muscle regeneration. *Cell Stem Cell* **4**, 217–225 (2009).
- Crist, C. G., Montarras, D. & Buckingham, M. Muscle satellite cells are primed for myogenesis but maintain quiescence with sequestration of Myf5 mRNA targeted by microRNA-31 in mRNP granules. *Cell Stem Cell* **11**, 118–126 (2012).
- Shea, K. L. et al. Sprouty1 regulates reversible quiescence of a self-renewing adult muscle stem cell pool during regeneration. *Cell Stem Cell* **6**, 117–129 (2010).
- Chakkalakal, J. V., Jones, K. M., Basson, M. A. & Brack, A. S. The aged niche disrupts muscle stem cell quiescence. *Nature* **490**, 355–360 (2012).
- Potten, C. S., Hume, W. J., Reid, P. & Cairns, J. The segregation of DNA in epithelial stem cells. *Cell* **15**, 899–906 (1978).
- Tumbar, T. et al. Defining the epithelial stem cell niche in skin. *Science* **303**, 359–363 (2004).
- Zambon, A. C. Use of the Ki67 promoter to label cell cycle entry in living cells. *Cytometry A* **77**, 564–570 (2010).
- Coller, H. A. What's taking so long? S-phase entry from quiescence versus proliferation. *Nat Rev Mol Cell Biol* **8**, 667–670 (2007).
- Sakaue-Sawano, A. et al. Visualizing spatiotemporal dynamics of multicellular cell-cycle progression. *Cell* **132**, 487–498 (2008).
- Sakaue-Sawano, A. et al. Tracing the silhouette of individual cells in S/G2/M phases with fluorescence. *Chem Biol* **15**, 1243–1248 (2008).
- Russo, A. A., Jeffrey, P. D., Patten, A. K., Massague, J. & Pavletich, N. P. Crystal structure of the p27Kip1 cyclin-dependent-kinase inhibitor bound to the cyclin A-Cdk2 complex. *Nature* **382**, 325–331 (1996).
- Toyoshima, H. & Hunter, T. p27, a novel inhibitor of G1 cyclin-Cdk protein kinase activity, is related to p21. *Cell* **78**, 67–74 (1994).
- Morgan, D. O. Principles of CDK regulation. *Nature* **374**, 131–134 (1995).
- Sherr, C. J. & Roberts, J. M. CDK inhibitors: positive and negative regulators of G1-phase progression. *Genes Dev* **13**, 1501–1512 (1999).
- Besson, A., Dowdy, S. F. & Roberts, J. M. CDK inhibitors: cell cycle regulators and beyond. *Dev Cell* **14**, 159–169 (2008).
- Kamura, T. et al. Cytoplasmic ubiquitin ligase KPC regulates proteolysis of p27(Kip1) at G1 phase. *Nat Cell Biol* **6**, 1229–1235 (2004).
- Hara, T. et al. Degradation of p27(Kip1) at the G(0)–G(1) transition mediated by a Skp2-independent ubiquitination pathway. *J Biol Chem* **276**, 48937–48943 (2001).
- Nakayama, K. et al. Skp2-mediated degradation of p27 regulates progression into mitosis. *Dev Cell* **6**, 661–672 (2004).
- Susaki, E., Nakayama, K. & Nakayama, K. I. Cyclin D2 translocates p27 out of the nucleus and promotes its degradation at the G0–G1 transition. *Mol Cell Biol* **27**, 4626–4640 (2007).
- Besson, A. et al. A pathway in quiescent cells that controls p27Kip1 stability, subcellular localization, and tumor suppression. *Genes Dev* **20**, 47–64 (2006).
- Coats, S., Flanagan, W. M., Nourse, J. & Roberts, J. M. Requirement of p27Kip1 for restriction point control of the fibroblast cell cycle. *Science* **272**, 877–880 (1996).
- Malek, N. P. et al. A mouse knock-in model exposes sequential proteolytic pathways that regulate p27Kip1 in G1 and S phase. *Nature* **413**, 323–327 (2001).



34. Vlach, J., Hennecke, S. & Amati, B. Phosphorylation-dependent degradation of the cyclin-dependent kinase inhibitor p27. *Embo J* **16**, 5334–5344 (1997).
35. Sauvageau, M. & Sauvageau, G. Polycomb group proteins: multi-faceted regulators of somatic stem cells and cancer. *Cell Stem Cell* **7**, 299–313 (2010).
36. Niwa, H., Yamamura, K. & Miyazaki, J. Efficient selection for high-expression transfectants with a novel eukaryotic vector. *Gene* **108**, 193–199 (1991).
37. Tamaki, T. *et al.* Identification of myogenic-endothelial progenitor cells in the interstitial spaces of skeletal muscle. *J Cell Biol* **157**, 571–577 (2002).
38. Qu-Petersen, Z. *et al.* Identification of a novel population of muscle stem cells in mice: potential for muscle regeneration. *J Cell Biol* **157**, 851–864 (2002).
39. Dreyfus, P. A. *et al.* Adult bone marrow-derived stem cells in muscle connective tissue and satellite cell niches. *Am J Pathol* **164**, 773–779 (2004).
40. Sharma, S. S., Ma, L., Bagui, T. K., Forinash, K. D. & Pledger, W. J. A p27Kip1 mutant that does not inhibit CDK activity promotes centrosome amplification and micronucleation. *Oncogene* **31**, 3989–3998 (2012).
41. Ono, R. *et al.* Dimerization of MLL fusion proteins and FLT3 activation synergize to induce multiple-lineage leukemogenesis. *J Clin Invest* **115**, 919–929 (2005).
42. Li, A. *et al.* Ciliary transition zone activation of phosphorylated Tctex-1 controls ciliary resorption, S-phase entry and fate of neural progenitors. *Nat Cell Biol* **13**, 402–411 (2011).
43. Ait-Si-Ali, S. *et al.* A Suv39h-dependent mechanism for silencing S-phase genes in differentiating but not in cycling cells. *EMBO J* **23**, 605–615 (2004).
44. Tsai, J. J. *et al.* Nrf2 regulates haematopoietic stem cell function. *Nat Cell Biol* **15**, 309–316 (2013).
45. Lankat-Buttgereit, B. & Goke, R. The tumour suppressor Pcd4: recent advances in the elucidation of function and regulation. *Biol Cell* **101**, 309–317 (2009).
46. Scortegagna, M., Martin, R. J., Kladney, R. D., Neumann, R. G. & Arbeit, J. M. Hypoxia-inducible factor-1alpha suppresses squamous carcinogenic progression and epithelial-mesenchymal transition. *Cancer Res* **69**, 2638–2646 (2009).
47. Helms, M. W. *et al.* TOB1 is regulated by EGF-dependent HER2 and EGFR signaling, is highly phosphorylated, and indicates poor prognosis in node-negative breast cancer. *Cancer Res* **69**, 5049–5056 (2009).
48. Nishimura, K. *et al.* APC(CDH1) targets MgcRacGAP for destruction in the late M phase. *PLoS One* **8**, e63001 (2013).
49. Kitamura, T. *et al.* Retrovirus-mediated gene transfer and expression cloning: powerful tools in functional genomics. *Exp Hematol* **31**, 1007–1014 (2003).
50. Morita, S., Kojima, T. & Kitamura, T. Plat-E: an efficient and stable system for transient packaging of retroviruses. *Gene Ther* **7**, 1063–1066 (2000).
51. Oki, T. *et al.* Aberrant expression of RasGRP1 cooperates with gain-of-function NOTCH1 mutations in T-cell leukemogenesis. *Leukemia* **26**, 1038–1045 (2012).
52. Kagiya, Y. *et al.* Upregulation of CD200R1 in lineage-negative leukemic cells is characteristic of AML1-ETO-positive leukemia in mice. *Int J Hematol* **96**, 638–648 (2012).
53. Bereshchenko, O. *et al.* Hematopoietic stem cell expansion precedes the generation of committed myeloid leukemia-initiating cells in C/EBPalpha mutant AML. *Cancer Cell* **16**, 390–400 (2009).
54. Subramanian, A. *et al.* Gene set enrichment analysis: a knowledge-based approach for interpreting genome-wide expression profiles. *Proc Natl Acad Sci U S A* **102**, 15545–15550 (2005).

Acknowledgments

We thank Mr. Tetsuya Tajima for technical assistance for imaging studies. We are grateful to Dr. Dovie Wylie for her excellent editing of English.

This work was supported by Grants-in-aid for Scientific Research on Innovative Areas, MEXT, Japan.

Author contributions

T.O. designed, performed all the experiments, and actively participated in manuscript writing. K.N., J.K., A.M., K.I. and K.T. technically supported in vitro and in vivo studies. A.S.S. and A.M. provided the plasmids and technically supported imaging studies. H.K. generated transgenic mice. K.T., K.A., A.N., S.M. and H.A. technically supported microarray analysis. T.K. conceived the project, secured funding and actively participated in writing the manuscript.

Additional information

Supplementary information accompanies this paper at <http://www.nature.com/scientificreports>

The GEO accession number for the microarray data reported in this paper is GSE46511.

Competing financial interests: The authors declare no competing financial interests.

How to cite this article: Oki, T. *et al.* A novel cell-cycle-indicator, mVenus-p27K⁻, identifies quiescent cells and visualizes G0–G1 transition. *Sci. Rep.* **4**, 4012; DOI:10.1038/srep04012 (2014).



This work is licensed under a Creative Commons Attribution-NonCommercial-NoDerivs 3.0 Unported license. To view a copy of this license, visit <http://creativecommons.org/licenses/by-nc-nd/3.0>